

Annealing Effect on Structure and Optical Properties of ZnO Thin Films Prepared by Spray Pyrolysis

Dr. Selma M.H. Al-Jawad 

Applied Sciences Department, University of Technology/Baghdad.

E-mail: Salma_Aljawad@yahoo.com

Received on: 25/8/2014 & Accepted on: 8/1/2015

ABSTRACT

Polycrystalline ZnO has been grown onto glass substrates by chemical spray pyrolysis (CSP) method. They were given heat treatment at different temperature and constant time and for different time with constant temperature in air. The change in structural and optical properties was studied by means of X-ray diffraction (XRD), SEM, and optical absorption measurements. Structural analysis by X-ray diffraction pattern showed annealed ZnO film has high-orientation along c - direction (0 0 2), which remained the same with different heat treatment. The lattice constants of ZnO thin films were also obtained from XRD data. It is found that, with the increase of different heat treatment, the lattice constant a increases from 3.208 Å to 3.254 Å, and c increases from 5.125 Å to 5.219 Å. where at higher annealing temperature and time the lattice constant c and a approach from bulk value. Other orientations corresponding to (1 0 0) and (1 0 1) are present with very low relative intensities as compared to that of (0 0 2) plane. The transparent is increasing with increasing annealing temperature and time due to decreasing in the films thickness with increasing annealing temperature and time. Change in bandgap energy from 3.2 to 3.01 eV was observed for different heat treatment.

تأثير التلدين على الخصائص الكهربائية والبصرية للأغشية الرقيقة ZnO المرسبة بطريقة الرش الكيميائي الحراري

الخلاصة

رسبت اغشية متعددة التبلور من ZnO على قواعد زجاجية بطريقة الرش الكيميائي الحراري (CSP). وتم اجراء معاملة حرارية للاغشية لدرجات حرارة مختلفة وزمن ثابت وكذلك لازمان تلدين مختلفة وعند درجة حرارة ثابتة في الهواء. درست الخصائص التركيبية والبصرية للاغشية باستخدام جهاز حيود الاشعة السينية (XRD), SEM, وقياسات الامتصاص البصري. ظهر من خلال فحص حيود الاشعة السينية ان الاغشية الملدنة تمتلك محور عالي عند الاتجاه (002) للمحور c , ويبقى التمحور نفسه لمختلف المعاملات الحرارية. وتم حساب معاملات الشبكة لاغشية ZnO من خلال بيانات حيود الاشعة السينية. حيث وجد انه بزيادة درجات حرارة التلدين او ازمان التلدين يزداد ثابت الشبكة a من 3.208 Å الى 3.254 Å, ويزداد ثابت الشبكة c من 5.125 Å الى 5.219 Å. حيث عند درجات حرارة التلدين العالية وازمان التلدين العالية يصبح ثابت الشبكة a و c قريب من قيم ثابت الشبكة الكتلي لاغشية ZnO. وظهرت كذلك قمم حيود عند ال (100) و (101) ولكن بشدة واطنة بالمقارنة مع المستوي (002). تزداد النفاذية بزيادة درجة حرارة التلدين وزمن التلدين نتيجة نقصان سمك الاغشية بزيادة درجة حرارة التلدين وزمن التلدين. وحصل تغير في فجوة الطاقة من 3.2 الى 3.01 eV نتيجة المعاملة الحرارية.

<https://doi.org/10.30684/etj.33.1B.14>

2412-0758/University of Technology-Iraq, Baghdad, Iraq

This is an open access article under the CC BY 4.0 license <http://creativecommons.org/licenses/by/4.0>

Keywords: ZnO, spray pyrolysis, structure, and optical properties.

INTRODUCTION

Wide bandgap materials such as GaN, ZnSe, ZnS, SiC, and ZnO have drawn great attention due to their applications in short wavelength photonic devices, window layers of hetero junction solar cells, transparent electrodes, and UV light emitting/receiving devices [1,2]. ZnO is one of the most promising material for fabricating optoelectronic devices that operate in the ultraviolet region, owing to its large exciton binding energy of 60 meV and wide band gap energy E_g of 3.37 eV at room temperature [3, 4], exhibiting many interesting electrical and optical properties [5], especially the recent discovery of ultraviolet luminescence at room temperature [6].

Different techniques were used to prepare ZnO thin films such as pulsed laser deposition[7-11], sputtering[12], chemical bath deposition[3,5,6,13,14], chemical-vapor deposition[15,16], sol gel[17,18], plasma-assisted molecular beam epitaxy[19], and chemical spray pyrolysis techniques[20-24]. Out of these, chemical spray pyrolysis (CSP) is an inexpensive low technology and safe method for producing highly transparent and conductive zinc oxide film [21].

V.R. Shinde et al. prepare textured ZnO thin films have been deposited using CBD method from aqueous alkaline medium, and are annealed in air at 623 K for 2 h[14]. Y. F. Lu et al. investigate the effects of thermal annealing on the film composition and the chemical bonding[8]. Harish Kumar Yadav et al. study of the influence of postdeposition annealing treatment on the structural and optical properties of rf sputtered $Zn_{1-x}Mn_xO$ thin films deposited on glass substrate at room temperature [25].

In this paper, we report on the systematic study of the influence of post deposition annealing treatment (at different annealing temperature for constant time and for different time at constant temperature) on the structural and optical properties of chemical spray pyrolysis (CSP) thin films deposited on glass substrate at 350 °C.

Experimental

The substrate used for deposits of ZnO thin films in this work is the microscopic glass slides (boro-silicate glass) with dimensions (76 x 21x 1) mm. It was cleaned by diluted HF, ethanol and distilled water, then dried and wiped by optical cleaning paper.

The ZnO films were prepared by using an aqueous solution of Zinc Chloride ($ZnCl_2 \cdot 2H_2O$) with molarity (0.1) M. The aqueous solution was diluted in distilled water and mixed by a magnetic stirrer, and in each deposition the volume used was (100 ml).

The ZnO thin films were deposited by spray pyrolysis technique. The deposition method involves the decomposition of an aqueous solution of zinc chloride. The spray solution was sprayed onto heated substrates held at $(573 \pm 5 \text{ }^\circ\text{K})$. Compressed air was used as a gas carrier and it was fed with the solution into a spray nozzle at a pre-adjusted constant atomization pressure.

The nozzle-to-substrate distance was 25 cm and the spraying period was (5 s) with flow rate as (3 ml/min).

Aluminum electrodes were evaporated on the surface of ZnO thin films using thermal evaporation equipment through a mask giving sensitive area $(0.5 \times 0.5) \text{ cm}^2$.

Ellipsometer equipped with a He-Ne laser source ($\lambda = 632.8$ nm) were conducted to calculate film thickness.

To determine the nature of the growth films and the structural characteristics of ZnO films, X – ray diffraction measurement has been done and compared with the ASTM (American Society of Testing Materials) cards, using Philips PW 1840 X – ray diffractometer of $\lambda_{\alpha} = 1.54 \text{ \AA}$ from Cu - K α . The average grain size (GS) of the polycrystalline material can be calculated from the X – ray spectrum by means of Full Width at Half Maximum (FWHM) method (Scherrer relation) [26].

$$GS = \frac{A \lambda}{\Delta \theta \cos \theta} \quad (2)$$

where

$\Delta \theta$ is the full – width at half maximum of the XRD peak appearing at the diffraction angle θ , A the shape factor, the value of which depends on the crystalline shape, and generally it is 1. For the (100) orientation the lattice constant a was calculated by [10]

$$a = \frac{\lambda}{\sqrt{3} \sin \theta} \quad (3)$$

for the (002) orientation the lattice constant c was calculated by

$$c = \frac{\lambda}{\sin \theta} \quad (4)$$

The morphology of the films was studied by Scanning Electron Microscopy (SEM) type VEGA TE SCAN equipment operated at 30 keV. UV-VIS, Phoenix-2000V device was used to record the optical transmission for ZnO/glass thin films annealing in the range (300 – 1100 nm). The data from transmission spectrum can be used in the calculation of the absorption coefficient (α) for ZnO films, according to the following equation [27]:

$$\alpha = \frac{1}{d} \ln \frac{1}{T} \quad (5)$$

Where d is the thickness of thin film, and T is the transmission.

In the direct band gap structure or direct transition semiconductors (present case), the absorption coefficient and optical band gap (E_g) are related by [28].

$$\alpha = (h\nu - E_g)^{1/2} \quad (6)$$

Where

h is Plank's constant and ν is the frequency of the incident photon.

The strain along the c axis, ε_{zz} is given by the following equation [17]

$$\varepsilon_{zz} = \frac{c_f - c_b}{c_b} \times 100\% \quad (7)$$

And the stress (σ_f) in the plane of the film has been calculated from the estimated value of lattice parameter of film (c_f) using the expression,[25]

$$\sigma_f = 4.5 \times 10^{12} (c_f - c_b) / c_b \quad (8)$$

Where

$c_b = 5.206$ (Å) is the lattice constant of bulk ZnO.

Results

Structures properties

The X-ray diffraction patterns of ZnO thin film deposited at 573 K are shown in figure (1) for different annealing temperature with constant time and for different time with constant temperature. Polycrystalline ZnO thin films show a preferred orientation in the (002) direction perpendicular to the substrate. Diffraction patterns preliminary recorded on the film indicated that all investigated films were polycrystalline for a range of 2θ from 20° to 80° at 1° glancing angle. The film was crystallized in the wurtzite phase and presents a preferential orientation along the c -axis, the strongest peak observed at $2\theta = 34.390^\circ$ ($d = 0.2605$ nm), Other orientations corresponding to (1 0 0) and (1 0 1) are present with very low relative intensities as compared to that of (0 0 2) plane. These results are close to those reported in the literature [14]. Also the intensity of (002) peak was much stronger than that of (101) orientation. This indicates that the c axis of the grains became uniformly perpendicular to the substrate surface, suggesting that the surface energy of (002) plane was the lowest in ZnO crystals. Some additional peaks with small intensities were detected with orientation 110, and 004 with mainly be due to heat treatment. As seen from figure, with increasing annealing temperature and time, the orientation along (0 0 2) has remained the same, but other orientations (1 0 0), (1 0 1), (110), and (004) have increased in their relative intensities.

The average grain size was calculated using Scherrer's formula (2), the values of average grain size show increases with increasing annealing temperature and time as shown in figure (2) it may be due to decrease in growth rate. The calculated grain size is smaller than grain size for ZnO deposited by pulsed laser deposition [8]. This result is consistent with the researcher Harish Kumar Yadav et al.[25]. The lattice constant a and c are obtained from equations (3) and (4) respectively. These are shown in Figure (3) as a function of annealing temperature and time, it is clear from figure that the lattice constant c continuously increases with an increase in the postdeposition annealing temperature and time. The defects in the form of interstitial oxygen present in the films annealed out at a higher annealing temperature, and the compressive forces become weaker, resulting the c -axis value approach from bulk of c -axis value with an increase in annealing temperature and time. The small value of lattice constant for the as grown and at low annealed samples compared to the unstressed powder value shows that the unit cell is elongated along the c axis, and compressive forces act in the plane of the film. Also we found at higher annealing temperature and time the lattice constant c and a approach from bulk value. The stress σ_f in the plane

of the film has been calculated from the estimated value of lattice parameter of film c_f using the equation 8. The estimated values of stress in the films are shown in Fig 4. The negative sign of estimated stress for all the samples indicates that the crystallites are in a state of compressive stress. However, the presence of interstitial oxygen has an expansive effect on the lattice, which results in the compressive strain, normally observed to occur along the c axis [25]. The table (1) show the obtained results. Figure (5) shows the scanning electron microscopy SEM micrographs for the films deposited on a glass substrate by using spray pyrolysis technique for ZnO films deposited at substrate temperature 573 k. ZnO forms 'blocks', tilted image gives more information about "blocks" shape.

Optical properties

Optical transmission spectra depend on the chemical and crystal structure of the films, and also on the film thickness and on films surface morphology. The effect of different annealing temperature and time on these spectra is shown in Figure (6). We have found that the films have high transmission at long wave lengths approximately (90%), and decreasing transmission to approximately (20%) at short wave lengths.

The transparent is increasing with increasing annealing temperature and time due to decreasing in the films thickness with increasing annealing temperature and time. These results are consistent with other published results such as results of Jong Hoon Kim et al.[7] who attributed the increasing in transmission for the preservation of the stoichiometry of the deposited polycomponent films. The crystallization of thin films strongly depends on the RTA temperature. At higher temperature, films have less impurities and it is the origin of varying of the electrical and optical properties.

The absorption coefficient (α) of ZnO films with different annealing temperature and time, determined from transmittance measurements using equation (5) shown inset figure (6). From this figure, the absorption coefficient of ZnO thin films decreased not sharply in the UV / VIS boundary and depends directly on the cut-off wavelength, and then decreased gradually in the visible region because it is inversely proportional to the transmittance.

The optical energy gap (E_g) value is calculated by extrapolation of the straight line of the plot of $(\alpha h\nu)^2$ versus photon energy for different annealing temperature and time as shown inset in Figure (7). The linear dependence of $(\alpha h\nu)^2$ with $(h\nu)$ indicates direct band gap. The annealed samples show a relative decrease in optical band gap with both annealing temperature and time Figure (7) the shift of band gap energy is related to the compressed lattice will provide a wider band gap because of the increased repulsion between the oxygen $2p$ and the zinc $4s$ bands. On the other hand, the stretched lattice can result in the narrowing of the band gap. This result is consistent with other researchers such as V.R. Shinde[14], Hong Seong Kang[9], and Harish Kumar Yadav[25]. The results of energy gap as a function of annealing temperature and time show in table (2).

Conclusions

ZnO (0 0 2) textured films with wurtzite crystal structure (confirmed from XRD) were obtained using chemical spray pyrolysis (CSP) method. The postdeposition annealing of ZnO film increases the grain size and reduces the presence of compressive stress. The band gap of ZnO films decreases slightly with annealing temperature and time. The improvement in disorder and the reduction in stress with postdeposition annealing of ZnO film gives a good optical and structural property.

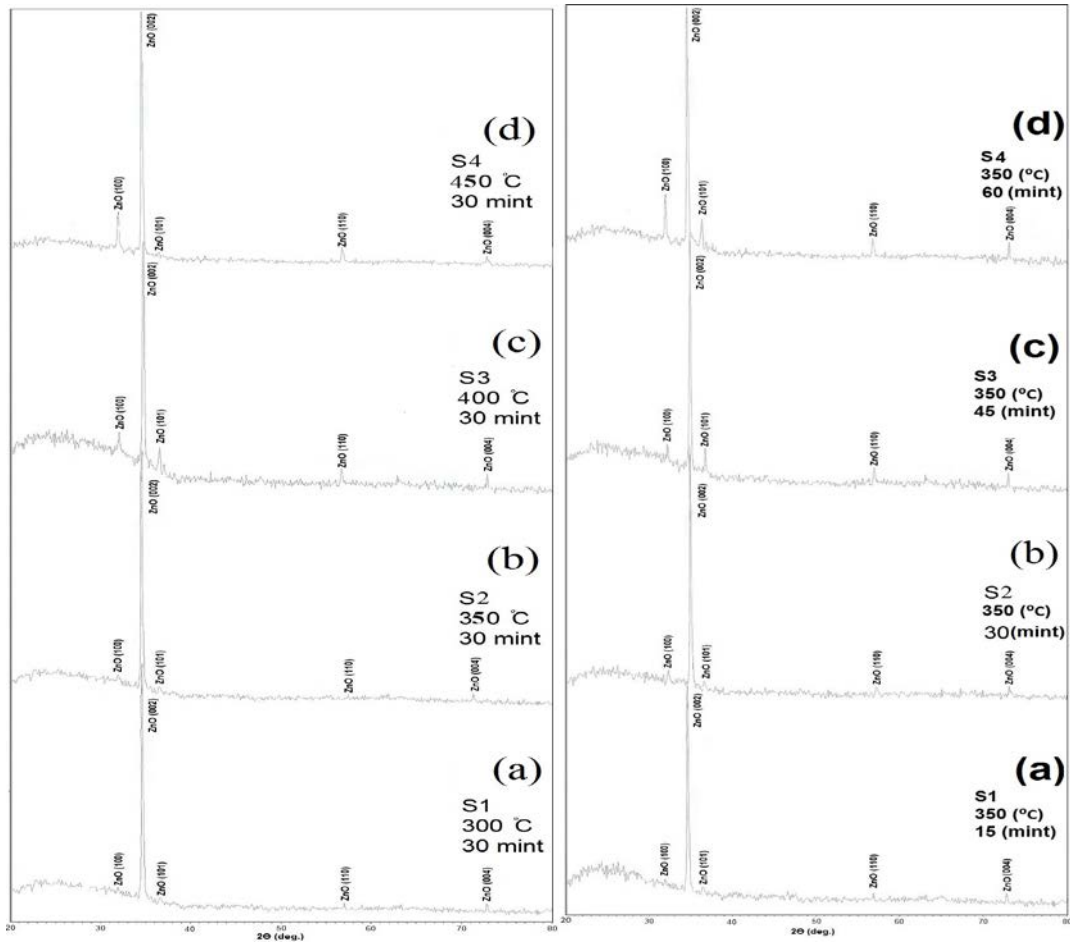


Figure (1) XRD of ZnO thin films (a) at different annealing temperature for constant time 30 min. (b) for different annealing time at constant temperature 350 °C.

Φ	β (deg)	N_L	g (A°)	Δ (deg)	d_{x-Ray} (A°)	d_{ASTM} (A°)	2θ X-Ray	c (A°)	a (A°)	2θ ASTM	Plain	Annealing time (mint)	Annealing temperature ($^\circ C$)	Sample
0.025	7.500	9.700	412	0.193	2.805	2.810	31.875	5.611	3.240	31.819	(100)	30	300	S1
0.012	16.000	9.760	410	0.193	2.605	2.610	34.390	5.212	3.009	34.330	(002)			
0.064	6.000	19.640	204	0.387	2.463	2.460	36.444	4.927	2.845	36.494	(101)			
0.025	7.500	10.620	377	0.193	1.611	1.610	57.100	3.224	1.861	57.166	(110)			
0.025	9.000	13.530	296	0.225	1.296	1.300	72.912	2.593	1.497	72.672	(004)			
0.035	4.500	7.500	535	0.161	2.800	2.810	31.935	5.601	3.234	31.819	(100)	30	350	S2
0.013	15.500	9.900	402	0.216	2.585	2.610	34.666	5.172	2.986	34.330	(002)			
0.026	13.500	16.200	246	0.354	2.465	2.460	36.419	4.931	2.847	36.494	(101)			
0.032	6.000	8.200	488	0.193	1.614	1.610	57.000	3.229	1.864	57.166	(110)			
0.038	5.000	7.500	532	0.193	1.298	1.300	72.800	2.596	1.499	72.672	(004)			
0.030	7.500	10.460	382	0.225	2.794	2.810	32.000	5.590	3.227	31.819	(100)	30	400	S3
0.016	13.500	10.390	385	0.225	2.585	2.610	34.666	5.172	2.986	34.330	(002)			
0.032	9.000	13.290	301	0.290	2.462	2.460	36.455	4.926	2.844	36.494	(101)			
0.022	10.000	9.570	418	0.225	1.619	1.610	56.806	3.239	1.870	57.166	(110)			
0.038	17.500	26.240	152	0.677	1.295	1.300	73.000	2.590	1.495	72.672	(004)			
0.024	8.000	8.970	446	0.193	2.813	2.810	31.774	5.629	3.250	31.819	(100)	30	450	S4
0.023	11.000	11.880	337	0.258	2.610	2.610	34.387	5.212	3.009	34.330	(002)			
0.039	6.500	11.820	338	0.258	2.460	2.460	36.258	4.952	2.859	36.494	(101)			
0.019	15.000	12.310	325	0.290	1.623	1.610	56.666	3.246	1.874	57.166	(110)			
0.040	4.000	6.260	639	0.161	1.300	1.300	72.612	2.602	1.502	72.672	(004)			
0.032	7.000	11.300	353	0.226	2.780	2.810	32.129	5.568	3.215	31.819	(100)	15	350	S5
0.011	17.000	9.800	409	0.194	2.573	2.610	34.840	5.147	2.971	34.330	(002)			
0.037	6.000	11.500	349	0.226	2.450	2.460	36.650	4.901	2.829	36.494	(101)			
0.032	15.000	26.500	151	0.484	1.613	1.610	57.050	3.226	1.863	57.166	(110)			
0.038	12.500	29.000	138	0.484	1.295	1.300	72.970	2.591	1.496	72.672	(004)			
0.019	11.500	11.300	353	0.226	2.778	2.810	32.193	5.557	3.208	31.819	(100)	45	350	S6
0.015	15.000	11.400	351	0.226	2.584	2.610	34.677	5.170	2.985	34.330	(002)			
0.043	13.500	29.500	136	0.581	2.458	2.460	36.516	4.918	2.839	36.494	(101)			
0.043	6.000	14.100	283	0.258	1.614	1.610	57.000	3.229	1.864	57.166	(110)			
0.016	8.000	7.700	517	0.129	1.295	1.300	73.000	2.590	1.495	72.672	(004)			

0.050	4.500	11.300	353	0.226	2.794	2.810	32.000	5.590	3.227	31.819	(100)	60	350	S7
0.023	12.500	14.600	273	0.290	2.594	2.610	34.548	5.189	2.996	34.330	(002)			
0.026	6.000	8.200	489	0.161	2.456	2.460	36.548	4.914	2.837	36.494	(101)			
0.032	7.000	12.400	323	0.226	1.616	1.610	56.935	3.232	1.866	57.166	(110)			
0.038	10.000	23.200	173	0.387	1.300	1.300	72.870	2.594	1.498	72.672	(004)			

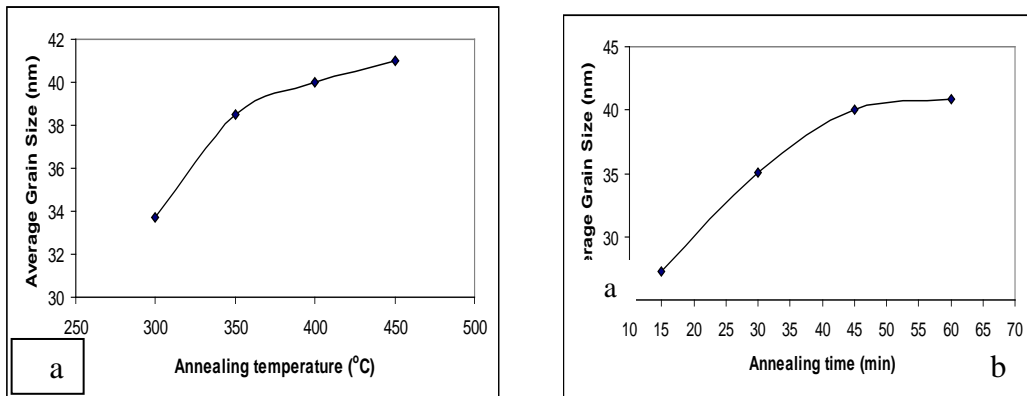


Figure (2) average grain size as a function of (a) annealing temperature. (b) Annealing time.

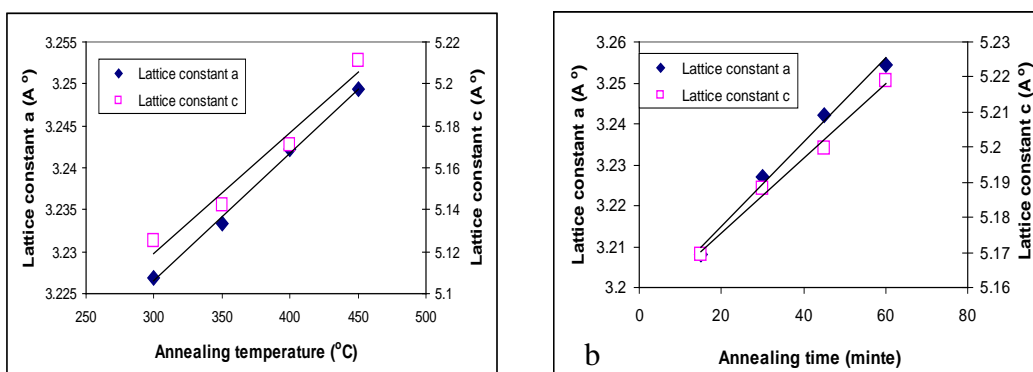


Figure (3) lattice constant a and c for the (002) and (100) orientation as a function of (a) annealing temperature (b) annealing time.

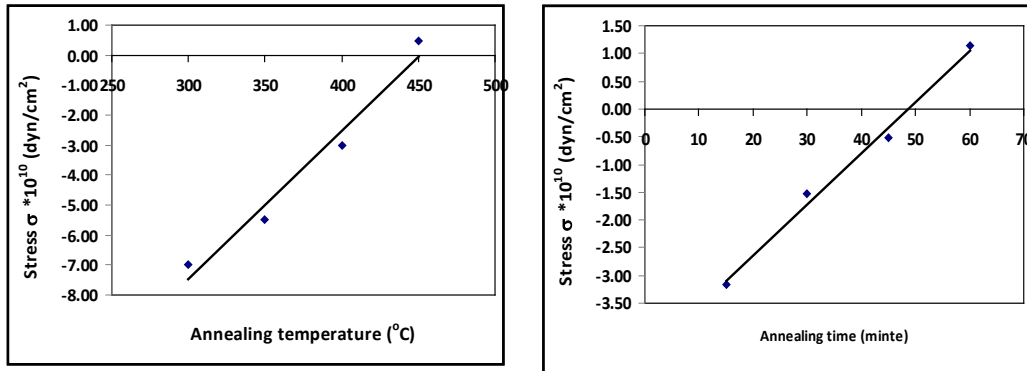


Figure (4) stress as a function of (a) annealing temperature (b) annealing time.

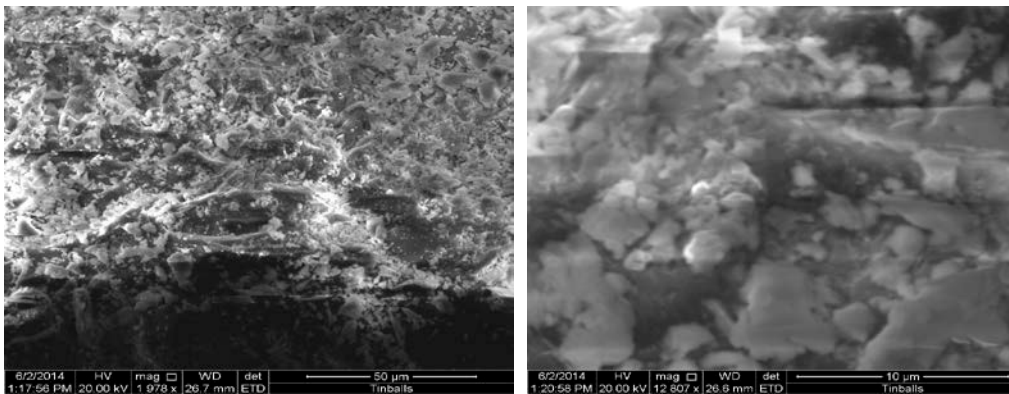


Figure (5): SEM image of ZnO thin film for different magnification.

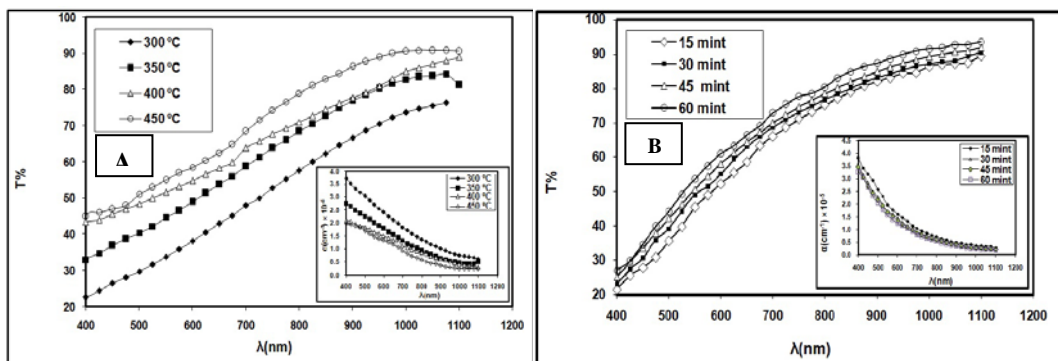


Figure (6) Transmittance spectra of ZnO thin films. (A) at different annealing temperature for constant time 30 min. (b) for different annealing time at constant temperature 350 °C. Inset shows Absorption Coefficient (α) as a Function of wavelength.

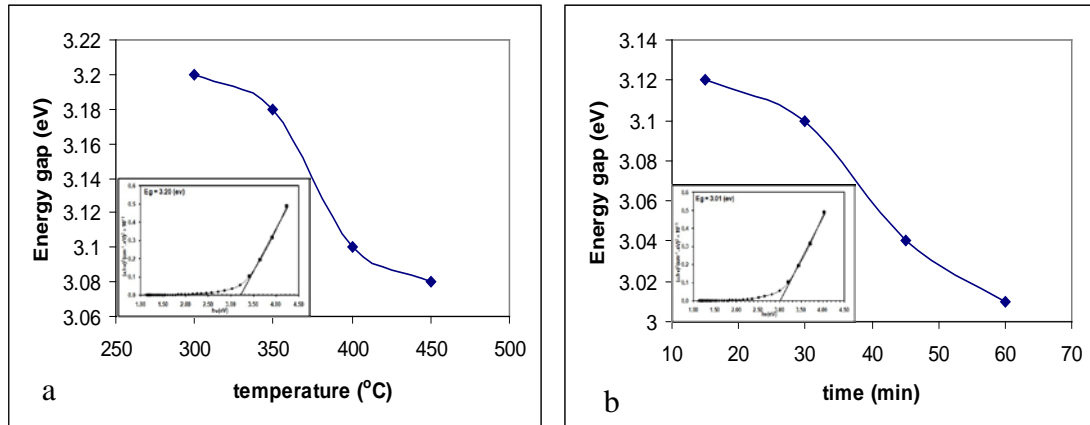


Figure (7) Band gap as a function (A) at different annealing temperature for constant time 30 min. (b) for different annealing time at constant temperature 350 °C. Inset Plots of $(\alpha h\nu)^2$ as a Function of Photon Energy.

Table (2)) The results of energy gap as a function of annealing temperature and time.

Temperature(°C)	Time (mint)	Energy band Eg (eV)
300	30	3.2
350	30	3.18
400	30	3.1
450	30	3.08
350	15	3.12
350	30	3.1
350	45	3.04
350	60	3.01

REFERENCE

[1] Tae Hyun Kim, Jin Jae Park, Sang Hwan Nam, Hye Sun Park, Nu Ri Cheong, Jae Kyu Song and Seung Min Park "Fabrication of Mg-doped ZnO thin films by laser ablation of Zn:Mg target" journal of Applied Surface Science 255 (2009) 5264–5266.
 [2] Masaki Azuma and Masaya Ichimura" Fabrication of ZnO thin films by the photochemical deposition method" journal of Materials Research Bulletin 43 (2008) 3537–3542.
 [3] Y. Lare , A. Godoy , L. Cattin , K. Jondo , T. Abachi , F.R. Diaz , M. Morsli , K. Napo , M.A. del Valle , J.C. Berne`de , " ZnO thin films fabricated by chemical bath deposition, used as buffer layer in organic solar cells" journal of Applied Surface Science 255 (2009) 6615–6619.
 [4] J. W. Shin and J. Y. Lee " Effects of thermal treatment on the formation of the columnar structures in ZnO thin films grown on p-Si „100... substrates" journal of APPLIED PHYSICS 100, 013526 (2006).

- [5] A.M. Peiro^a, C. Domingob, J. Peral^a, X. Dome`nech^a, E. Vigil^c, M.A. Herna´ndez-Fenollosad, M. Mollar^d, B. Mari^d, J.A. Ayllon^{a,*} " Nanostructured zinc oxide films grown from microwave activated aqueous solutions" journal of Thin Solid Films 483 (2005) 79– 83.
- [6] X.D. Gao, X.M. Li, W.D. Yu " Structural and morphological evolution of ZnO cluster film prepared by the ultrasonic irradiation assisted solution route" journal of Thin Solid Films 484 (2005) 160– 164.
- [7] Jong Hoon Kim, Byung Du Ahn, Choong Hee Lee, Kyung Ah Jeon, Hong Seong Kang, and Sang Yeol Lee, "Effect of rapid thermal annealing on electrical and optical properties of Ga doped ZnO thin films prepared at room temperature" JOURNAL OF APPLIED PHYSICS 100, 113515 (2006).
- [8] Y. F. Lu, H. Q. Ni, Z. H. Mai, and Z. M. Ren " The effects of thermal annealing on ZnO thin films grown by pulsed laser deposition" JOURNAL OF APPLIED PHYSICS VOLUME 88, NUMBER 1. 2000.
- [9] Hong Seong Kang, Jeong Seok Kang, Jae Won Kim, and Sang Yeol Lee^{a)} "Annealing effect on the property of ultraviolet and green emissions of ZnO thin films" OF APPLIED PHYSICS VOLUME 95, NUMBER 3. 2004.
- [10] F. K. Shan,^{a)} B. I. Kim, G. X. Liu, Z. F. Liu,^{b)} J. Y. Sohn, W. J. Lee, B. C. Shin, and Y. S. Yu^{c)} " Blueshift of near band edge emission in Mg doped ZnO thin films and aging" JOURNAL OF APPLIED PHYSICS VOLUME 95, NUMBER 9 (2004).
- [11] Nguyen Hoa Hong, Joe Sakai, and Awatef Hassini, " Magnetic properties of V-doped ZnO thin films", JOURNAL OF APPLIED PHYSICS, Vol. **97**, 2005.
- [12] F. Couzinié-Devy , N. Barreau, and J. Kessler, "Dependence of ZnO:Al properties on the substrate to target position in RF sputtering", Thin Solid Films, Vol. 516, 2008, 7094–7097.
- [13] Zhiguang Wang, Minqiang Wang, Zhonghai Lin, Yaohui Xue, Ge Huang, and Xi Yao, " Growth and interconversion of ZnO nanostructure films on different substrates", Applied Surface Science, Vol. 255 , 2009, 4705–4710.
- [14] V.R. Shinde, C.D. Lokhande, R.S. Mane, Sung-Hwan Han, "Hydrophobic and textured ZnO films deposited by chemical bath deposition: annealing effect" journal of Applied Surface Science, Vol. 245 ,2005, 407–413.
- [15] X. T. Zhang, Y. C. Liu,^{a)} L. G. Zhang, J. Y. Zhang, Y. M. Lu, D. Z. Shen, W. Xu, G. Z. Zhong, X. W. Fan, and X. G. Kong, " Structure and optically pumped lasing from nanocrystalline ZnO thin films prepared by thermal oxidation of ZnS thin films" JOURNAL OF APPLIED PHYSICS Vol. 92, N. 6, 15, 2002.
- [16] B. S. Li, Y. C. Liu,^{a)} Z. S. Chu, D. Z. Shen, Y. M. Lu, J. Y. Zhang, and X. W. Fan, " High quality ZnO thin films grown by plasma enhanced chemical vapor deposition", JOURNAL OF APPLIED PHYSICS, Vol. 91, N. 11, 2002.
- [17] R. Ghosh, D. Basak, and S. Fujihara, " Effect of substrate-induced strain on the structural, electrical, and optical properties of polycrystalline ZnO thin films", JOURNAL OF APPLIED PHYSICS, Vol. 96, N. 5 , 2004.
- [18] Litty Irimpan, D. Ambika, V. Kumar, V. P. N. Nampoori, and P. Radhakrishnan, " Effect of annealing on the spectral and nonlinear optical characteristics of thin films of nano-ZnO", JOURNAL OF APPLIED PHYSICS, Vol. 104, 2008.
- [19] Shujie Jiao, Youming Lu, Zhengzhong Zhang, Binghui Li, Bin Yao, Jiying Zhang, Dongxu Zhao, Dezhen Shen, and Xiwu Fan, " Optical and electrical properties of highly nitrogen-doped ZnO thin films grown by plasma-assisted molecular beam epitaxy", JOURNAL OF APPLIED PHYSICS, Vol. 102, 2007.

- [20] Sh. U. Yuldashev, a_ G. N. Panin, and T. W. Kang ,R. A. Nusretov and I. V. Khvan," Electrical and optical properties of ZnO thin films grown on Si substrates", JOURNAL OF APPLIED PHYSICS Vol. 100, 2006.
- [21] P. M. Ratheesh Kumar, C. Sudha Kartha, and K. P. Vijayakumar," Doping of spray-pyrolyzed ZnO thin films through direct diffusion of indium: Structural optical and electrical studies" journal of APPLIED PHYSICS, Vol. 98, 2005.
- [22] M. Krunk , T. Dedova, I. Oja Açıık," Spray pyrolysis deposition of zinc oxide nanostructured layers, Thin Solid Films, Vol. 515 ,2006, 1157–1160.
- [23] Raid A. Ismail , Selma M. H. Al-Jawad, and Naba Hussein," Preparation of n-ZnO/p-Si solar cells by oxidation of zinc nanoparticles: effect of oxidation temperature on the photovoltaic properties", Applied Physics A Material Science and Processing, Vol. 117, 2014, 1977–1984.
- [24] Abdeslam DOUAYAR, Hassan BIHRI, Ahmed Mzerd Azzam, BELAYACHI and 1 Mohammed ABD-LEFDIL," Structural, Optical and Electrical Properties of Transparent Conducting Oxide Based on Al Doped ZnO Prepared by Spray Pyrolysis", Sensors & Transducers, Vol. 27, 2014, pp. 156-160.
- [25] Harish Kumar Yadav, K. Sreenivas, and Vinay Gupta^{a)} " Influence of postdeposition annealing on the structural and optical properties of cosputtered Mn doped ZnO thin films" JOURNAL OF APPLIED PHYSICS 99, 083507 (2006).
- [26] B.D. Cullity and S.R. Stock, "Elements of X – Ray Diffraction", Third edition, Prentice-Hall in the United States of America, 2011.
- [27] S.M. Sze, "Physics of Semiconductor Devices", Second edition, Jon Wiley and Sons, New York, 1981.
- [28] S. Dimitrijevic, "Understanding Semiconductor Devices", Copyright by Oxford University Press, 2000.